COMPUTER METHODS IN MATERIALS SCIENCE

2021, vol. 21, no. 1, 25–34
https://doi.org/10.7494/cmms.2021.1.0743

A numerical simulation study of mold filling in the injection molding process

Markus Baum*, Denis Anders

Cologne University of Applied Sciences (TH Köln), Group for Computational Mechanics and Fluid Dynamics, Steinmüllerallee 1, 51643 Gummersbach, Germany.

Abstract

Injection molding can undoubtedly be regarded as one of the most widely used manufacturing processes for polymers (Guevara-Morales & Figueroa-Lopez, 2014). Furthermore, injection molding has found its way into various branches of industry (Fernandez et al., 2018) since it has several essential advantages over other processing techniques in terms of good surface finish, the ability to process complex parts without the need for secondary operations, and low cost for mass production. In order to find optimal process settings, it is necessary to gain a deeper insight into the filling process and the underlying physical phenomena, as well as a thorough understanding of the complex material behavior. In this context, the numerical simulation of the injection molding process is increasingly important. Therefore, the current contribution is dedicated to present a thorough comparative numerical study for the mold filling of an exemplary thin-walled mold geometry, including a realistic non-Newtonian viscosity model for the polymer melt. For the numerical simulation, the authors employ the commercial CFD software packages Cadmould 3D-F and ANSYS CFX. While ANSYS CFX is a well-established CFD software for numerical modelling of multiphysical phenomena, Cadmould 3D-F is a highly specialized and computationally efficient alternative suitable for certain geometric configurations in the context of injection molding. The present study is new in the sense that it demonstrates the equivalence of the considered software packages for the simulation of the injection molding process in thin-walled mold geometries.

Keywords: injection molding, polymers, Hele-Shaw approximation, computational fluid dynamics, computing methods

1. Introduction

In the course of globalization, injection molding (IM) has seen rapid technological development and opened up new fields of application for electronic components devices, medical devices as well as in the automotive/transport industry and packaging industry. Alongside extrusion, injection molding is one of the most important primary forming manufacturing processes in the plastics processing industry.

The growing competition on the global market for plastic products results in increased demands on process efficiency and product quality. In the context of injection molding, mass homogeneity and high dimensional accuracy, minimization of shrinkage and warpage, surface structure (degree of gloss and the surface quality), and strength properties (e.g., fiber orientation for glass fiber reinforced plastics) are typical indicators for product quality.

Optimization of product quality, on the one hand, while minimizing process costs on the other requires an in-depth understanding of the injection molding process. In this context, injection molding simulation plays an essential role. The main objective is to determine the influence of adjustable process variables such as mold cavity characteristics, gating and temperature control system,

* Corresponding author: markus.baum@th-koeln.de
ORCID ID's: 0000-0001-5840-1374 (M. Baum), 0000-0002-7849-0666 (D. Anders)

volume flow, process pressure, and temperatures, etc. on the relevant quality indicators like cycle time, dimensional accuracy, shrinkage/distortion, energy consumption, etc. The results of the simulation consequently serve as a basis for subsequent iterative optimization of the process using statistical methods of data analysis, e.g. design of experiment (DOE), artificial neural network (ANN), and machine learning techniques (ML). Figure 1 illustrates the basic scheme of this iterative optimization process.

As already mentioned, the application of simulation software for injection molding is an important instrument in the optimization procedure. Since the optimization process usually involves numerous iteration steps, which in turn requires injection molding simulations at each step, the computational efficiency and precision of the employed simulation packages essentially determine the efficiency of the overall optimization procedure. Therefore, the current paper focuses on a detailed comparative numerical study of mold filling in an exemplary thin-walled mold geometry including a realistic non-Newtonian viscosity model for the polymer melt. The high numerical precision of ANSYS CFX software package for the simulation of mold filling is undisputed and has already been validated against experimental studies (Mukras & Al-Mufadi, 2016; Rusdi et al., 2016). Unfortunately, the high computational cost of simulations in ANSYS CFX makes it impractical for extensive parametric optimization. This results in an acute demand for rapid numerical approaches that are accurate and robust at the same time.

For this reason, the rest of this contribution is organized as follows. After presenting a brief introduction into some of the fundamentals of the injection molding process in section 2, a special focus is placed in section 3 on the mathematical modelling and approximation strategies for the geometry as well as for the governing set of partial differential equations. In order to present a vivid example of an application for the two introduced simulation strategies an exemplary filling study in a thin-walled rectangular geometry with real material parameters is given in sections 4 and 5. A short summary and outlook in section 6 conclude the paper.

2. Fundamentals of the injection molding process

First of all, let us take a closer look at the fundamentals of the injection molding process. As illustrated in Figure 2, an injection molding machine can be subdivided into two basic units. In the plasticizing unit, the polymer granulate is fed into the machine and heated to melting temperature. Then, the liquid polymer is injected through a nozzle at high pressure into the cavity of a mold, which is located in the clamping unit. This cavity defines the geometric shape of the final product.

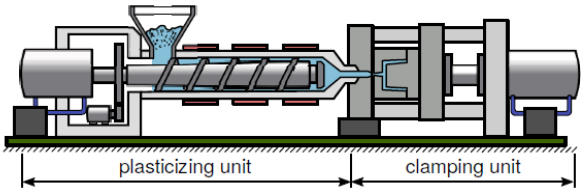

Fig. 2. An illustration of an injection molding machine

After the volumetric filling of the mold cavity, the polymer is first compressed due to its compressibility before it cools and solidifies. As soon as sufficient stiffness is reached to allow for demolding, the mold is opened, and the injection-molded part is ejected.

The main advantages of the injection molding process over other manufacturing processes result from the extremely fast and automated production process as well as cost-effective production of complex molded parts in large quantities. Additionally, further finishing of the molded parts is usually not necessary.

The major disadvantages of the injection molding process are caused by the relatively high manufacturing costs for the molds compared to the actual process. For this reason, subsequent modifications to the mold are extremely expensive and need to be prevented by thorough numerical investigations in the early stages of product design as well as the cooling strategy.

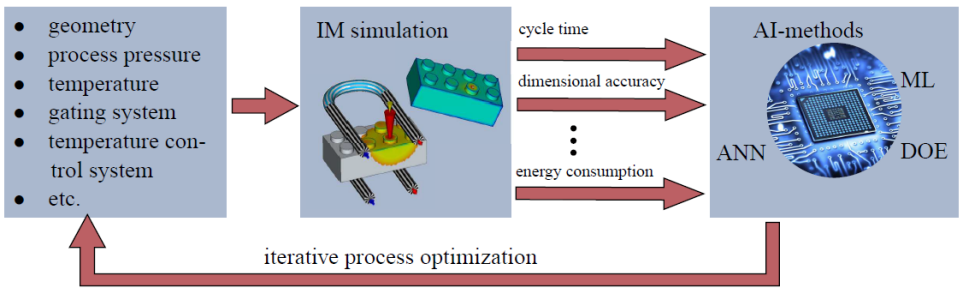

Fig. 1. Scheme for an optimization process in injection molding

The injection molding process is characterized by some special challenges such as component optimization and process-compatible design, optimization of gating systems for balanced filling of single and multiple cavities, adjustment of an accurate or low-error filling characteristic, process control close to the optimum operating point, and design of a suitable temperature control layout for the injection mold.

In the context of this contribution, the authors put a special emphasis on the filling phase since the filling characteristic has a significant influence on the product quality.

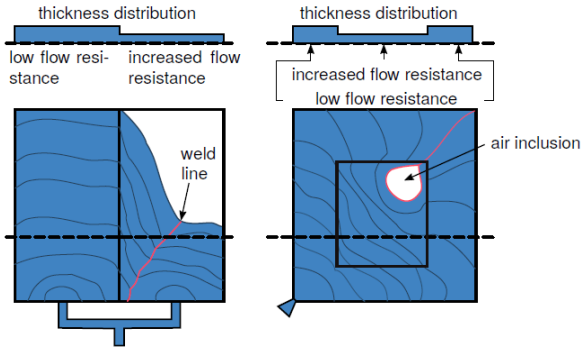

Fig. 3. The effects of thickness changes on the filling process

As shown in Figure 3, different thickness distributions induce inhomogeneous flow resistances. In turn, these can lead to typical filling problems like weld lines or air inclusions. A balanced filling process avoiding filling problems is a very demanding task, especially for complex geometries as well as for multiple cavities. To this end, numerical filling studies need to be employed in the early stages of product development and mold design.

The filling process has also a strong impact on the heat transfer within the cavity, cf. Figure 4. Inhomogeneous filling conditions due to different flow velocities and shear stresses within the cavity usually induce inhomogeneous heat transfer conditions. This can ultimately cause strongly pronounced geometric distortion as well as shrinkage and warpage.

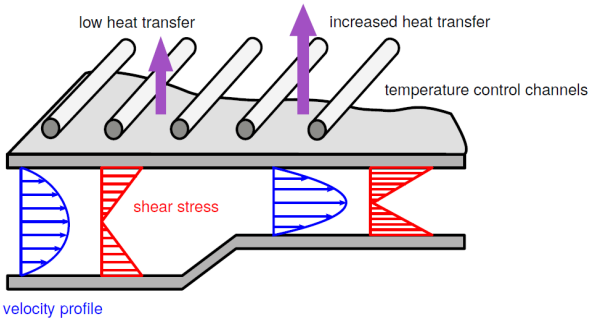

Fig. 4. The effects of thickness changes on the heat transfer

3. Mathematical modelling of the injection molding process

In the mathematical modelling of the injection molding process, there are two predominant approaches, a full volumetric and a semi-volumetric approach, respectively. In the 3D full volumetric modelling of the cavity, the volume is spatially discretized by using the finite volume method and the full set of Navier–Stokes equations as governing equations (Mukras & Al-Mufadi, 2016; Rusdi et al., 2014; Zhang et al., 2016). In the semi-volumetric framework, so-called 2.5D modelling approaches are employed. The semi-volumetric model is replaced by a suitable surface or mid-plane model (Cardozo, 2009). The surfaces are transformed into a 2D finite element mesh, and the volume is discretized via networks of bar elements (Simcon Kunststofftechnische Software GmbH, 2004). These different discretization strategies according to Studer and Ehring (2013) are illustrated in Figure 5.

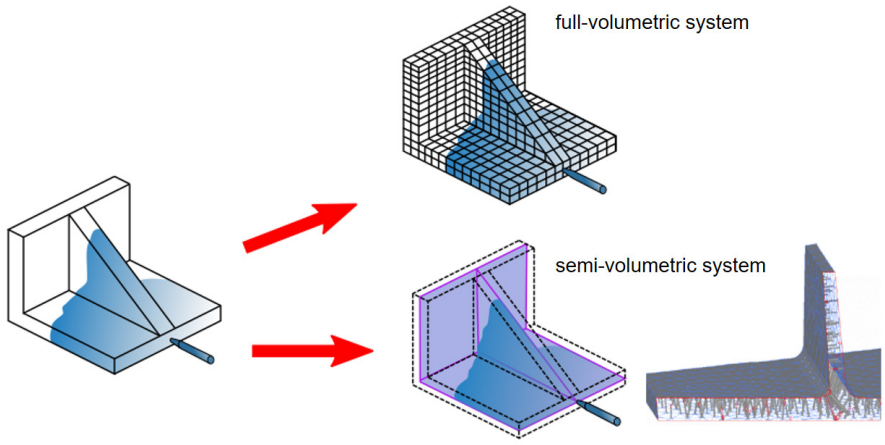

Fig. 5. The modelling approaches of a full volumetric and a semi-volumetric system

In the full volumetric modelling, the complete Navier–Stokes equations including the mass balance are considered during the filling phase:

$$\frac{\partial \rho}{\partial t} + \nabla \cdot \left(\rho \vec{u}\right) = 0 \tag{1}$$

$$\frac{\partial}{\partial t}\left(\rho \vec{u}\right) + \nabla \cdot \left(\rho \vec{u} \otimes \vec{u} + p \cdot I - \eta\left(\nabla \vec{u} + \nabla \vec{u}^{T}\right)\right) = \rho \vec{g} \tag{2}$$

For the thermal analysis, the equations (1) and (2) are coupled with the energy balance:

$$\rho c_p \left(\frac{\partial T}{\partial t} + \vec{u} \cdot \nabla T\right) = \nabla\left(\lambda \nabla T\right) + \eta \dot{\gamma}^2 \tag{3}$$

In the scope of semi-volumetric modelling, a generalized Hele-Shaw approximation of the Navier–Stokes equations is used for the filling phase (Hieber & Shen, 1980):

$$\frac{\partial \rho}{\partial t} + \frac{\partial}{\partial x}\left(\rho u\right) + \frac{\partial}{\partial y}\left(\rho v\right) = 0 \tag{4}$$

$$\frac{\partial p}{\partial x} = \frac{\partial}{\partial z}\left(\eta \frac{\partial u}{\partial z}\right) \tag{5}$$

$$\frac{\partial p}{\partial y} = \frac{\partial}{\partial z}\left(\eta \frac{\partial v}{\partial z}\right) \tag{6}$$

The Hele-Shaw approximation is usually motivated by the small wall thickness of injection molded components (Hele-Shaw, 1899). The associated energy balance is simplified in this formulation to:

$$\rho c_p \left(\frac{\partial T}{\partial t} + u \frac{\partial T}{\partial x} + v \frac{\partial T}{\partial y}\right) = \lambda \frac{\partial^2 T}{\partial z} + \eta \dot{\gamma}^2 \tag{7}$$

In the Hele-Shaw approximation, the shear strain rate is formulated to:

$$\dot{\gamma} = \sqrt{\left(\frac{\partial u}{\partial z}\right)^2 + \left(\frac{\partial v}{\partial z}\right)^2} \tag{8}$$

The z-coordinate characterizes the wall thickness of the mold cavity.

The viscosity of polymer melts depends in a highly nonlinear way on the shear rate $\dot{\gamma}$. Due to the shear-thinning (pseudoplastic) behavior, polymer melts belong to the non-Newtonian liquids. Formally, it applies $\eta = f(T, p, \dot{\gamma})$.

Various models have been developed for the mathematical description of viscosity behavior. The most common viscosity models in injection molding simulation are the Cross-WLF model and the Carreau-WLF model, cf. work by Osswald and Rudolph (2015). In the Cross-WLF model, the viscosity is determined according to (Kaiser et al., 2012):

$$\eta\left(T, p, \dot{\gamma}\right) = \frac{\eta_0\left(T, p\right)}{1 + \left(\frac{\eta_0\left(T, p\right)\dot{\gamma}}{\tau^*}\right)^{1-n}} \tag{9}$$

This equation is characterized by the reference viscosity η_0, the critical shear stress τ^* and the power-law index n. The reference viscosity is given by Hieber (1987):

$$\eta_0 = D_1 \cdot \exp\left[\frac{-A_1\left(T - D_2 - D_3 \cdot p\right)}{\tilde{A}_2 + T - D_2}\right] \tag{10}$$

The viscosity in the Carreau-WLF model is given by Karrenberg et al. (2013):

$$\eta\left(T, p, \dot{\gamma}\right) = \frac{\alpha_T\left(T, p\right) \cdot P_1}{\left(1 + P_2 \cdot \dot{\gamma} \cdot \alpha_T\left(T, p\right)\right)^{P_3}} \tag{11}$$

where α_T is the temperature shift factor, P_1 is the reference viscosity, P_2 is the reciprocal transition velocity and P_3 the slope of the viscosity curve in the pseudo-plastic viscosity range. The temperature shift factor follows from the WLF equation and can be described by Karrenberg et al. (2013), and Nielsen and Landel (1994):

$$\lg\left(\alpha_T\right) = \frac{C_1\left(T_0 - T_S\right)}{C_2 + \left(T_0 - T_S\right)} - \frac{C_1\left(T - T_S\right)}{C_2 + \left(T - T_S\right)} \tag{12}$$

Thermal shrinkage is compensated for in the holding-pressure phase. In this phase, the cavity is completely filled with the melt and further melt is pressed into the cavity due to its compressibility. For the modelling of the compressibility, the equation of state (pvT-relationship) is used. There are different approaches to describing the equation of state, e.g., Spencer-Gilmore or Tait model (Chiang et al., 1991; Fernandez et al., 2018). For the simulation of polymers, the modified Tait model is given by:

$$v\left(p, T\right) = v_0\left(T\right)\left[1 - C \cdot \ln\left(1 + \frac{p}{B\left(T\right)}\right)\right] + v_t\left(p, T\right) \tag{13}$$

where $C = 0.0894$.

This equation of state is describing the liquid and the solid regions of a polymer by the specific volume at zero gauge pressure $v_0(T)$ and pressure sensitivity of the material $B(T)$.

The melt region ($T > T_t$) can be described by the following equations (Chiang et al., 1991):

$$v_0(T) = b_{1m} + b_{2m}(T - b_5) \tag{14}$$

$$B(T) = b_{3m} \cdot \exp\left[-b_{4m}(T - b_5)\right] \tag{15}$$

$$v_t(p,T) = 0 \tag{16}$$

Here b_{1m}, b_{2m}, b_{3m}, b_{4m} and b_5 are data fitted coefficient of the model.

For the description of the solid region ($T < T_t$), the following equations can be used (Chiang et al., 1991):

$$v_0(T) = b_{1s} + b_{2s}(T - b_5) \tag{17}$$

$$B(T) = b_{3s} \cdot \exp\left[-b_{4s}(T - b_5)\right] \tag{18}$$

$$v_t(p,T) = b_7 \cdot \exp\left[b_8(T - b_5) - b_9 p\right] \tag{19}$$

Here b_{1s}, b_{2s}, b_{3s}, b_{4s}, b_5, b_7, b_8 and b_9 are data fitted coefficient of the model.

The transition temperature between the liquid and the solid state is given by (Chiang et al., 1991; Fernandez et al., 2018):

$$T_t(p) = b_5 + b_6 p \tag{20}$$

In the simulation of shrinkage and warpage, it is necessary to calculate the residual stresses of the molded part. The residual stresses are results from the thermally induced shrinkage and the inhomogeneous cooling. The behavior of viscoelastic materials can be described by an anisotropic linear thermo-viscoelastic model (Rezayat & Stafford, 1991):

$$\sigma_{ij} = \int_0^t C_{ijkl}\left(\xi(t) - \xi(t')\right) \cdot \left(\frac{\partial \varepsilon_{kl}}{\partial t'} - \alpha_{th,kl}\frac{\partial T}{\partial t'}\right) \mathrm{d}t' \tag{21}$$

In this equation, the stress tensor and the strain tensor are described as σ_{ij} and ε_{kl}, respectively (Studer & Ehring, 2013). These stresses are result from a temporal accumulation of the thermal and mechanical strain components (Studer & Ehring, 2014). $\alpha_{th,kl}$ is a tensor for the linear thermal expansion and C_{ijkl} is describing the elasticity of the fourth stage. The time-scale $\xi(t)$ is given by (Fernandez et al., 2018):

$$\xi(t) := \int_0^t \frac{1}{\alpha_T}\,\mathrm{d}t' \tag{22}$$

4. The numerical simulation model of the filling process

For the numerical simulation of the filling process, a thin-walled cavity is used. The particular interest lies in the evaluation of the temporal flow front evolution. Geometry with a thickness of 2.1 mm, a width, and a length of 62 mm was used. A circular inlet area with a diameter of 1.1 mm was provided on the geometry, and the cavity has a constant wall temperature of 80°C, see Figure 6. The first material is the polymer Schulamid 66 SK 1000, and the second is air with the relevant material parameters are considered. The values for the material density, thermal conductivity, specific heat capacity, and thermal diffusivity are listed in Table 1. They are taken from the internal Cadmould 3D-F material library.

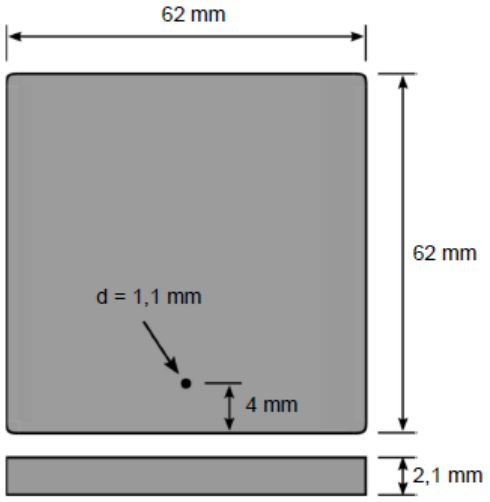

Fig. 6. A sketch of the geometry for the mold filling

Table 1. Material properties for the polymer and the air

Material	Property	Value
polymer	density (solid)	1060 kg/m^3
polymer	density (melt)	860 kg/m^3
polymer	thermal conductivity	0.28 W/(m · K)
polymer	specific heat capacity	1700 J/(kg · K)
polymer	thermal diffusivity	0.19 mm^2/s
air	density (gas)	1.185 kg/m^3
air	dynamic viscosity	$1.831 \cdot 10^{-5}$ kg/(m · s)
air	thermal conductivity	$2.61 \cdot 10^{-2}$ W/(m · K)
air	specific heat capacity	1004.4 J/(kg · K)

In this simulation, the Carreau-WLF model is used to describe the polymer viscosity, and the relevant material parameters are provided in Table 2.

Table 2. Data used for viscosity description in numerical modelling with the Carreau-WLF model

Parameter	Value
P_1	900.83269 Pa·s
P_2	0.026588668 s
P_3	0.50322362
T_0	290°C
T_s	128.72119°C
C_1	8.86
C_2	101.6

For the simulation of the filling process in ANSYS CFX an inhomogeneous multi-phase model is used (Haagh & Van De Vosse, 1998). In order to prevent air inclusions, it is important to enable a free-slip boundary condition for the air on the cavity wall. The boundary condition for the polymer can be prescribed as a no-slip wall (Mukras & Al-Mufadi, 2016). The inlet boundary conditions were set up with a constant mass flow rate for the halved geometry of $\dot{m} = 0.0086$ kg/s. For a better calculation time a halved geometry with a symmetry plane was used for the modelling. The outlet is defined as an opening with a static pressure of $p_{stat} = 0$ bar.

In Cadmould 3D-F the boundary conditions are automatically set as no slip walls. In order to guarantee a two dimensional inlet geometry, a short hot runner must be defined at the inlet. The inlet has an equivalent volume flow rate of $\dot{V} = 20$ cm^3/s and temperature. The outflow of the air is calculated automatically by an internal code.

Both models using a constant inlet temperature of $T = 280$°C and a constant cavity wall temperature of $T = 80$°C. These models are shown in Figure 7.

The mesh for the CFD simulation is a full-volumetric mesh and is build up in ANSYS CFX. The mesh consists of tetrahedra, pyramids, and wedges with 299.115 elements in total. The maximum element size is 0.5 mm, and the mesh is prepared with 5 inflation layers at the walls. In Cadmould 3D-F the mesh is build up by an internal mesh generator with 66.224 elements and a maximum element size of 0.9 mm. The mesh is a semi-volumetric mesh with triangular surface elements. The slightly varying mesh sizes result from different discretization strategies within ANSYS CFX and Cadmould 3D-F. Both meshes are shown in Figure 8.

Based on the Cadmould 3D-F time step size in ANSYS CFX an adaptive time step control with a maximum time step of 10^{-3} s was selected. In ANSYS CFX the residual convergence target for all equations was set at 10^{-5} with a maximum iteration of 50.

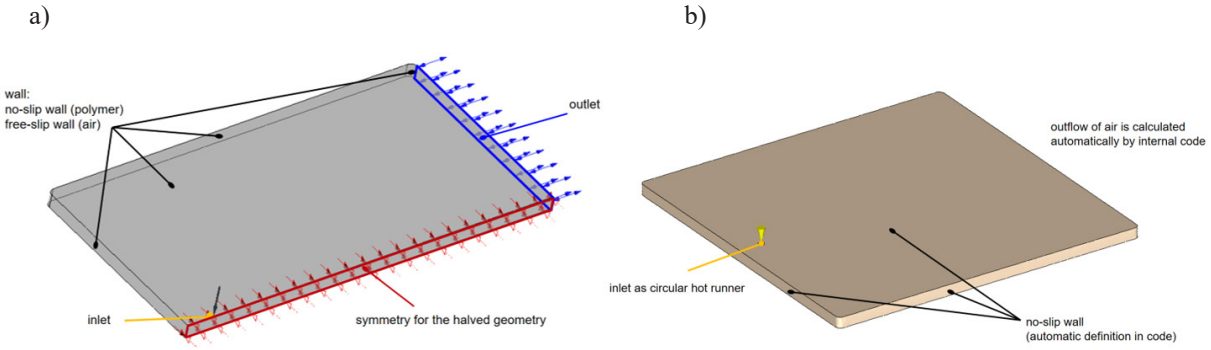

Fig. 7. Simulation models in ANSYS CFX (a) and Cadmould 3D-F (b)

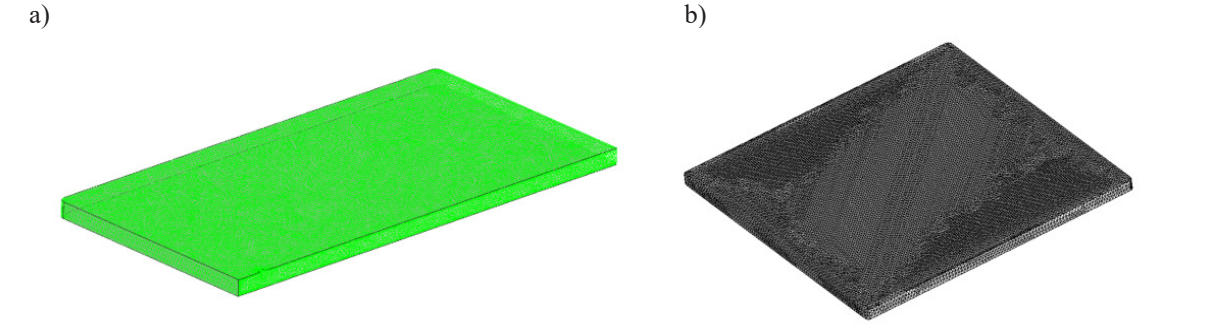

Fig. 8. Meshes in ANSYS CFX (a) and Cadmould 3D-F (b)

5. The results of the numerical simulation study

The simulation results demonstrate that the flow front of the polymer melt is initially characterized by the geometry and the inflow process as shown in Figure 9. The comparison is made for the different time steps. Due to the 2.5D method in Cadmould 3D-F, a smooth flow front is formed. However, ANSYS CFX has slightly sharp edges on the flow front, which are created by the influence of small eddies at the inlet.

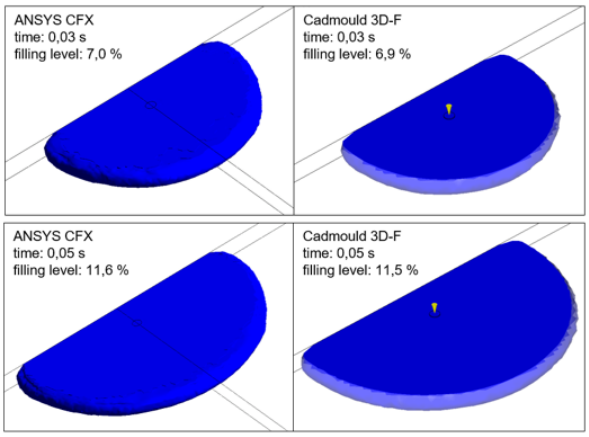

Fig. 9. Results for the early filling phase at the time steps 0.03 s and 0.05 s

Between the time steps 0.1 s and 0.2 s the polymer melt contacts the sidewalls of the cavity and the evolution of a larger flow front can be observed, cf. Figure 10. The subsequent filling phase at the time step 0.3 s is characterized by a constant progression of the polymer melt. It can be seen that the flow front of the melt is very similar for all time steps with slight variation in the filling level.

Figure 11 shows a temporal shape of the flow front within the mid plane of the cavity. Booth simulation strategies show a good agreement at the evolution of the flow front. Only on the cavity wall is the melt front slightly different. In Cadmould 3D-F the influence of the boundary conditions is more pronounced than in ANSYS CFX.

All simulations were performed on a 3.1 GHz Intel Xeon E5-2687W v3 machine with 10 cores / 20 threads and 32 GBytes RAM. For ANSYS CFX, a multicore (HPC license) 2020 R1 license was employed. For the simulation in Cadmould 3D-F, a singlecore V13 license was used. While the computations in ANSYS CFX were completed after 62 hours and 47 minutes, the simulation in Cadmould 3D-F converged in 11 minutes and 31 seconds. The large difference in computation times is mainly caused by the different numerical approaches and discretization strategies in ANSYS CFX and Cadmould 3D-F. In terms of the simulation of the mold filling, both software packages provide almost equivalent results. Here, the results in ANSYS CFX serve as a reference for the validation of Cadmould 3D-F.

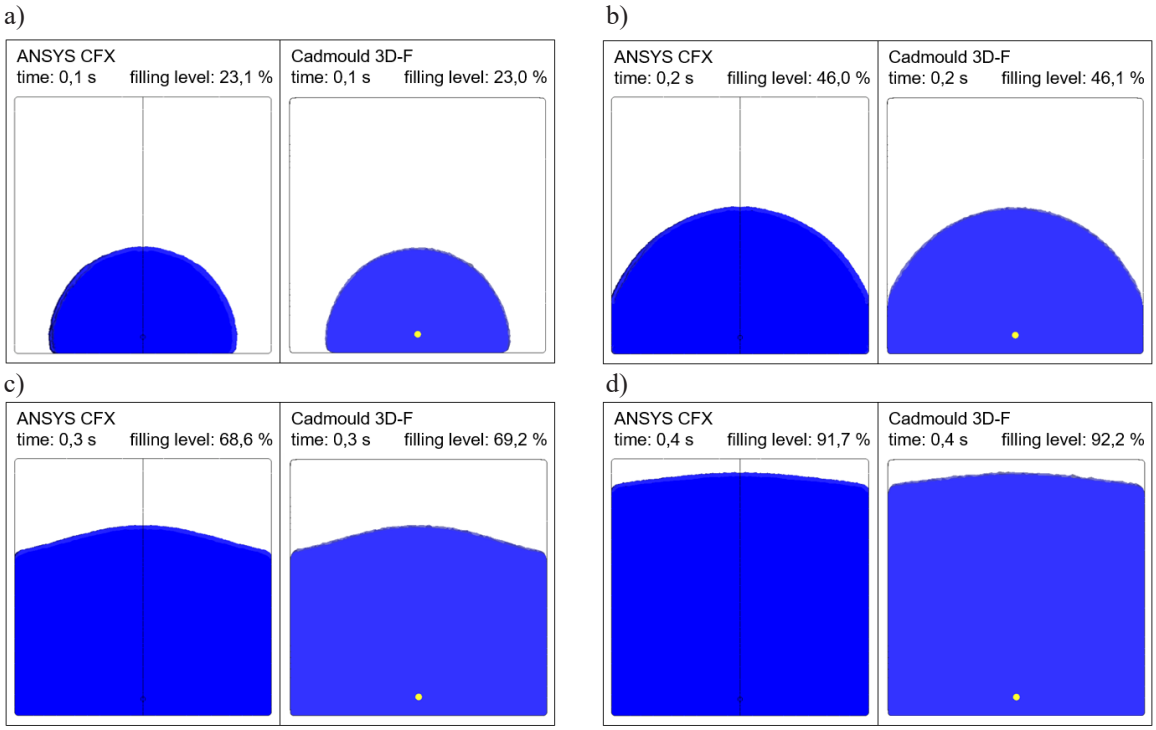

Fig. 10. Results of the filling phases between the simulations with ANSYS CFX (left) and Cadmould 3D-F (right): a) result at the time step 0.1 s; b) result at the time step 0.2 s; c) result at the time step 0.3 s; d) result at the time step 0.4 s

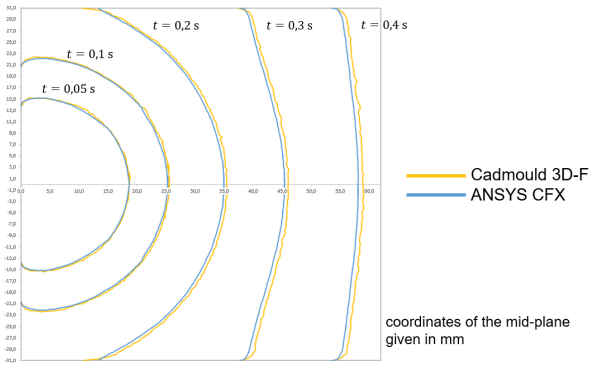

Fig. 11. A temporal evolution of the flow front within the mid plane of the cavity

6. Conclusion and outlook

This contribution demonstrates that the Hele-Shaw approximation employed in the Cadmould 3D-F framework offers a well suited, efficient, and sufficiently accurate simulation of the filling process in thin-walled structures. The simulation results of the full-volumetric model in ANSYS CFX and the semi-volumetric model in Cadmould 3D-F are almost equivalent. It can be observed that there are only slight differences in the contact areas between the polymer melt and the cavity walls. The reason for this can be found in the different setup of the boundary conditions at the wall and the characterization of the flow front. In full-volumetric models approaches, the fountain flow regime in the flow front is captured, while in the semi-volumetric approach, this effect is neglected. Another reason is that surface tension has certain effects on the flow front. This has been discussed by Wang et al. (2012). Due to the enormous time savings of calculations in Cadmould 3D-F compared to simulations in ANSYS CFX, Cadmould 3D-F may serve as a very efficient simulation tool for the iterative parameter optimization in injection molding processes. For the next research activities, the authors plan to make further validation of the simulation results with experimental filling studies as well as the implementation of a surrogate-assisted optimization procedure for injection molding including simulations in Cadmould 3D-F.

Acknowledgements

This contribution was developed within the OptiTemp project. The OptiTemp research project (reference number 13FH012PX8) is partly funded by the German Federal Ministry of Education and Research (BMBF) within the FHprofUnt 2018 research program.

References

Cardozo, D. (2009). A brief history of the filling simulation of injection moulding. *Journal of Mechanical Engineering Science*, *223*(3), 711–721. https://doi.org/10.1243/09544062JMES986.

Chiang, H.H., Hieber, C.A., & Wang, K.K. (1991). A Unified Simulation of the Filling and Postfilling Stages in Injection Molding. Part I: Formulation. *Polymer Engineering and Science*, *31*(2), 116–124. https://doi.org/10.1002/pen.760310210.

Fernandez, C., Pontes, A.J., Viana, J.C., & Gaspar-Cunha, A. (2018). Modelling and optimization of the injection-molding process: a review. *Advances in Polymer Technology*, *37*(2), 429–449. https://doi.org/10.1002/adv.21683.

Guevara-Morales, A., & Figueroa-López, U. (2014). Residual stresses in injection molded products. *Journal of Materials Science*, *49*, 4399–4415. https://doi.org/10.1007/s10853-014-8170-y.

Haagh, G.A.A.V., & Van De Vosse, F.N. (1998). Simulation of three dimensional polymer mould filling processes using a pseudo concentration method. *International Journal for Numerical Methods in Fluids*, *28*(9), 1355–1369. https://doi.org/10.1002/(SICI)1097-0363(19981215)28:9<1355::AID-FLD770>3.0.CO;2-C.

Hele-Shaw, H.S. (1899). The Motion of a Perfect Liquid. *Proceedings of the Royal Institution of Great Britain*, *16*, 49–64.

Hieber, C.A. (1987). Melt viscosity characterization and its application to injection molding. In A.I. Isayev (Ed.), *Injection and Compression Molding Fundamentals* (pp. 124–129). Marcel Dekker.

Hieber, C.A., & Shen, S.F. (1980). A Finite-Element/Finite-Difference Simulation of the Injection-Molding Filling Process. *Journal of Non-Newtonian Fluid Mechanics*, *7*(1), 1–32. https://doi.org/10.1016/0377-0257(80)85012-9.

Kaiser, J.-M., Arab, A., & Stommel, M. (2012). Device to Determine Rheological Properties of Thermoplastics Blended with Chemical Foaming Agent. *Zeitschrift Kunststofftechnik / Journal of Plastics Technology*, *8*, 91–105.

Karrenberg, G., Neubrech, B., & Wortberg, J. (2013). CFD-Simulation der Kunststoffplastifizierung in einem Extruder mit durchgehend genutetem Zylinder und Barriereschnecke. *Zeitschrift Kunststofftechnik / Journal of Plastics Technology*, *12*(3), 205–238. https://doi.org/10.3139/O999.04032016.

Mukras, S.M.S., & Al-Mufadi, F.A (2016). Simulation of HDPE Mold Filling in the Injection Molding Process with Comparison to Experiments. *Arabian Journal for Science and Engineering*, *41*(5), 2847–2856. https://doi.org/10.1007/s13369-015-1970-9.

Nielsen, L.E., & Landel, R.F. (1994). *Mechanical Properties of Polymers and Composites*. Marcel Dekker.

Osswald, T.A., & Rudolph, N. (2015). *Polymer rheology. Fundamentals and applications*. Hanser Publications.

Rezayat, M., & Stafford, R.O. (1991). A thermoviscoelastic model for residual stress in injection molded thermoplastics. *Polymer Engineering and Science*, *31*(6), 393–398. https://doi.org/10.1002/pen.760310602.

Rusdi, M.S., Abdullah, M.Z., Mahmud, A.S., Khor, C.Y., Abdul Aziz, M.S., Abdullah, M.K., Yusoff, H., & Firdaus, S.M. (2014). Numerical Investigation on the Effect of Injection Pressure on Melt Front Pressure and Velocity Drop. *Applied Mechanics and Material*, *786*, 210–214. https://doi.org/10.4028/www.scientific.net/AMM.786.210.

Rusdi, M.S., Abdullah, M.Z., Mahmud, A.S., Khor, C.Y., Abdul Aziz, M.S., Ariff, Z.M., & Abdullah, M.K. (2016). Numerical Investigation on the Effect of Pressure and Temperature on the Melt Filling During Injection Molding Process. *Arabian Journal for Science and Engineering*, *41*(5), 1907–1919. https://doi.org/10.1007/s13369-016-2039-0.

Simcon Kunststofftechnische Software GmbH (2004). Simulation of fluid flow and structural analysis within thin walled three dimensional geometries, *European Patent Application*, EP 1385103 A1.

Studer, M., & Ehring, F. (2013). Reduktion von Formteilverzug beim Spritzgießen durch optimale Wanddickenverteilung – Eine Machbarkeitsstudie. *Zeitschrift Kunststofftechnik / Journal of Plastics Technology*, *9*, 209–252.

Studer, M., & Ehring, F. (2014). Minimizing Part Warpage in Injection Molding by Optimizing Wall Thickness Distribution. *Advances in Polymer Technology*, *33*(S1), 21454. https://doi.org/10.1002/adv.21454.

Wang, W., Li, X., & Han, X. (2012). Numerical simulation and experimental verification of the filling stage in injection molding. *Polymer Engineering and Science*, *52*(1), 42–51. https://doi.org/10.1002/pen.22043.

Zhang, J., Yin, X., Liu, F., & Yang, P. (2016). The simulation of the warpage rule of the thin-walled part of polypropylene composite based on the coupling effect of mold deformation and injection molding process. *Science and Engineering of Composite Materials*, *25*(3), 593–601. https://doi.org/10.1515/secm-2015-0195.